International Journal of Pharmaceutics 358 (2008) 271–277

Contents lists available at ScienceDirect

International Journal of Pharmaceutics

journal homepage: www.elsevier.com/locate/ijpharm

Pharmaceutical Nanotechnology

Preparation and biodisposition of methoxypolyethylene glycol amine–poly (DL-lactic acid) copolymer nanoparticles loaded with pyrene-ended poly(DL-lactic acid)

Masanaho Sasatsu, Hiraku Onishi*, Yoshiharu Machida

Department of Drug Delivery Research, Hoshi University, 2-4-41, Ebara, Shinagawa-ku, Tokyo 142-8501, Japan

ARTICLE INFO

Article history:
Received 13 November 2007
Received in revised form 28 January 2008
Accepted 3 March 2008
Available online 18 March 2008

Keywords:
PLA–(MeO-PEG) nanoparticle
PLA-pyrene
Biodisposition
Normal mice
Tumor-bearing mice

ABSTRACT

A formyl group-ended poly(DL-lactic acid) (PLA-aldehyde), synthesized in the same manner as reported previously, was utilized to produce the polymeric marker for PLA-related nanoparticles. Namely, pyrene-ended poly(DL-lactic acid) (PLA-pyrene) was prepared as a polymeric marker by the reductive amination of PLA-aldehyde and aminopyrene. Methoxypolyethylene glycol amine–poly(DL-lactic acid) block copolymer (PLA–(MeO-PEG) nanoparticles loaded with PLA-pyrene were prepared, and examined on retention of PLA-pyrene in the nanoparticles, and biodisposition in normal and sarcoma-180 solid tumor-bearing mice. PLA-pyrene was retained stably in PLA–(MeO-PEG) nanoparticles in a PBS-ethanol (7:3, v/v) mixture and a plasma-PBS (1:1, v/v) mixture, indicating that PLA-pyrene might be a useful marker of PLA–(MeO-PEG) nanoparticles themselves. After i.v. injection in normal rats, the plasma level of PLA-pyrene was very high for initial 8 h, and accumulated gradually into organs, especially spleen and liver. After i.v. injection in tumor-bearing mice, similar biodistribution profiles of PLA-pyrene were observed, and PLA-pyrene was accumulated well in tumor, suggesting that PLA–(MeO-PEG) nanoparticles should be delivered efficiently to solid tumors. It is suggested that PLA-pyrene might be a useful probe of the nanoparticles themselves. In addition, it was demonstrated that PLA–(MeO-PEG) nanoparticles should be a useful drug carrier for passive tumor targeting.

1. Introduction

Although hydrophobic antitumor agents such as camptothecin (CPT) or paclitaxel are strongly effective, their use is not easy due to their poor water solubility and severe toxic side effects; however, drug carrier systems may facilitate administration, improve efficacy and reduce toxic side effects. Recently, drug carriers like polymeric nanoparticles, liposomes, solid–lipid nanoparticles have been extensively investigated to optimize medication with antitumor agents, including drug targeting (Yang et al., 1999; Nagasaki et al., 2001; Charrois and Allen, 2004; Brannon-Peppas and Blanchette, 2004; Shenoy et al., 2005; Abraham et al., 2005). Our research group has been studying about PLA or PLGA-based micro- or nanoparticles, and demonstrated that nanoparticles prepared using the mixture of poly(DL-lactic acid) (PLA) and poly(ethylene glycol)-block-poly(propylene glycol)-block-poly(ethylene glycol) (PEG-PPG-PEG) or with methoxypolyethylene glycol–PLA block copolymer (MeO-PEG–PLA) were useful to improve the efficacy of irinotecan (CPT-11) or CPT (Onishi et al., 2003; Machida et al., 2003; Miura et al., 2004). In MeO-PEG–PLA nanoparticles, PLA chains form the core and PEG chains are located outside (Gref et al., 1994; Bazile et al., 1995). MeO-PEG–PLA nanoparticles can carry hydrophobic antitumor agents in their core, and their MeO-PEG shell can prevent interaction of the PLA core with biomolecules, cell and tissues (Dunn et al., 1997; Mosqueira et al., 1999), and can suppress opsonization (Nguyen et al., 2003). The particle size, electrical charge and surface structure of the drug carriers affect the biological behavior of nanoparticles (Sugibayashi et al., 1979; Kanke et al., 1980; Unezaki et al., 1995; Tabata et al., 1998; Ishida et al., 1999). Polymeric nanoparticles with a diameter of some dozen up to 400 nm and a hydrophilic surface generally tend to reside for a long time in the systemic circulation and to localize in diseased parts such as a solid tumor based on the enhanced permeability and retention (EPR) effect (Matsumura and Maeda, 1986; Jain, 1987; Yokoyama et al., 1991; Woodle and Lasic, 1992; Unezaki et al., 1995; Zhang et al., 1997). Accordingly, when nanoparticles with a hydrophilic surface are used as carriers for antitumor agents, the agents are expected to accumulate efficiently into the target, leading to high antitumor effect and less toxic side effects.

In the previous study, we synthesized PLA with a formyl terminal end, named PLA-aldehyde, as a reactive intermediate so that various types of PLA derivatives could be prepared,

* Corresponding author. Tel.: +81 3 5498 5724; fax: +81 3 3787 0036.
E-mail address: onishi@hoshi.ac.jp (H. Onishi).

0378-5173/$ – see front matter © 2008 Elsevier B.V. All rights reserved.
doi:10.1016/j.ijpharm.2008.03.011

and obtained methoxypolyethylene glycol amine–poly(DL-lactic acid) block copolymer (PLA–(MeO-PEG)) by reductive amination between PLA-aldehyde and methoxypolyethylene glycol amine (MeO-PEG(*N*)) (Sasatsu et al., 2005). In the present study, a PLA derivative was prepared as a florescent marker-labeled PLA by reductive amination between aminopyrene and PLA-aldehyde. The obtained novel probe (PLA-pyrene), expected as a probe of PLA–(MeO-PEG) nanoparticles, was examined on its retention in the nanoparticles by the incubation in the ethanol-buffer or plasma-buffer mixture. Furthermore, PLA–(MeO-PEG) nanoparticles loaded with PLA-pyrene were investigated for biodistribution using normal and sarcoma-180 tumor-bearing mice.

2. Materials and methods

2.1. Materials

3,3-Diethoxy-1-propanol, stannous octoate, methoxypolyethylene glycol amine (MeO-PEG(*N*)) and aminopyrene were purchased from Sigma–Aldrich Co. (St. Louis, MO, USA). DL-Lactide was obtained from Tokyo Kasei Kogyo Co., Ltd. (Japan). All other chemicals used were of reagent grade.

2.2. Animal and tumor

Male ddY mice (6–7 weeks old, 30 g) were purchased from Tokyo Laboratory Animals Science Co., Ltd. (Japan), and soon used for animal experiments. They were kept on the breeding diet MF (Oriental Yeast, Japan) with water ad libitum at room temperature maintained at 23 ± 1 °C and a relative humidity of 60 ± 5%. The experimental protocol was approved by the Committee on Animal Research of Hoshi University, Tokyo, Japan, and the animal experiments were performed in compliance with Guiding Principles for the Care and Use of Laboratory Animals, Hoshi University, Japan. Sarcoma-180 cells were kindly supplied by Cell Resource Center for Biomedical Research of Tohoku University (Japan) and used as tumor cells. The tumor cells were maintained by intraperitoneal transplantation to mice. Sarcoma-180 cell (1×10^6 cells) suspended in Hank's balanced solution (0.1 mL) were inoculated subcutaneously to each mouse at its axillary region to obtain tumor-bearing mice.

2.3. Polymer synthesis

(1) Acetal-ended poly(DL-lactic acid) (PLA-acetal) was synthesized with ring-opening polymerization, and aldehyde-ended poly(DL-lactic acid) (PLA-aldehyde) was obtained by acidic hydrolysis of PLA-acetal according to a previous paper (Sasatsu et al., 2005). Briefly, after 6 g of DL-lactide purified by recrystallization from an ethyl acetate solution and 3,3-diethoxy-1-propanol (50 mg) were placed in a three-neck flask filled with nitrogen gas in advance, 45 mL of toluene was added, and the mixture was stirred and heated on an oil bath set at 160 °C with stirring. After the mixture reached a set temperature, a toluene solution (5 mL) of stannous octoate (30 mg) was added. Then, the reflux was continued at a set temperature with stirring for 5 h, after which the mixture was left at room temperature for 24 h. The solvent was evaporated at 60 °C under reduced pressure, 120 mL of dichloromethane was added to the residue, and the mixture was filtrated with a glass filter. The filtrate was put into 200 mL of water stirred at 60 °C, and the dichloromethane was evaporated. The precipitate was obtained by filtration, redissolved in dichloromethane, and dried on anhydrous sodium sulfate. After the sodium sulfate was removed by filtration, the filtrate was evaporated to dryness to yield PLA-acetal. Although the product contained pure PLA/acetal (1:1, mol/mol) conjuagte and PLA, the product was named PLA-acetal. PLA-acetal was used in the next step without further purification. (2) PLA-aldehyde was obtained by acidic hydrolysis of PLA-acetal. PLA-acetal (200 mg) was dissolved in 80 mL of acetone, and 2% (w/v) hydrochloric acid (30 mL) was added. The mixture was stirred at room temperature for 24 h, and acetone was removed by evaporation to precipitate the product. After the supernatant was removed, the precipitate was dissolved in 80 mL of acetone. Then, 2% (w/v) hydrochloric acid (30 mL) was added to the solution, and the stirring and precipitation were repeated twice in the same way. The final precipitate was washed with water, and dried under reduced pressure to yield PLA-aldehyde. Although the product contained pure PLA/aldehyde (1:1, mol/mol) conjugate and PLA, the mixture was named PLA-aldehyde. PLA-aldehyde was used in the following experiments without further purification. (3) Methoxypolyethylene glycol amine–poly(DL-lactic acid) block copolymer (PLA–(MeO-PEG)) was obtained by reductive amination between PLA-aldehyde and MeO-PEG(*N*), as reported before (Sasatsu et al., 2005). Briefly, PLA-aldehyde (200 mg), MeO-PEG(*N*) (300 mg) and sodium cyanoborohydride (25 mg) were put in 25 mL of a mixture of dichloromethane and methanol (1:1, v/v), and the mixture was stirred at room temperature for 24 h, when the pH of the mixture was adjusted to 6–7 with 0.1 mol/mL hydrochloric acid aqueous solution and 0.1 mol/mL sodium hydroxide aqueous solution. After organic solvents were evaporated, the resultant suspension was lyophilized. Then, chloroform was added to the product, and the supernatant was subjected to gel permeation chromatography (GPC), and the fractions appearing before MeO-PEG(*N*) were collected. The collected fractions were evaporated, and then the residue was dissolved in acetone. The solution was suspended by the addition of water, and acetone was evaporated. The suspension was washed by ultrafiltration using a membrane with a MW cut off limit of 10,000. This sequential operation of dissolution, precipitation and ultrafiltration was repeated twice. The final aqueous suspension was lyophilized to yield PLA–(MeO-PEG). Although the product was the mixture of pure PLA/(MeO-PEG) (1:1, mol/mol) block copolymer and PLA, it was named PLA–(MeO-PEG)). PLA–(MeO-PEG) was used in the following experiments without further purification.

2.4. Synthesis of PLA-pyrene

Pyrene-ended poly(DL-lactic acid) (PLA-pyrene) was synthesized using almost the same method as PLA–(MeO-PEG) (Sasatsu et al., 2005) (Fig. 1). PLA-aldehyde (700 mg), aminopyrene (60 mg)

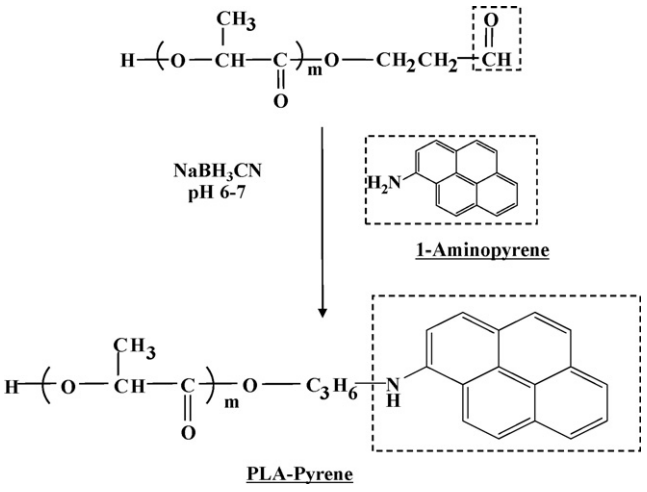

Fig. 1. Synthesis and chemical structure of PLA-pyrene.

and sodium cyanoborohydride (82 mg) were put in 77 mL of a mixture of dichloromethane and methanol (1:1, v/v), and the mixture was stirred at room temperature for 24 h, when the pH of the mixture was adjusted to 6–7 with 0.1 mol/mL hydrochloric acid aqueous solution and 0.1 mol/mL sodium hydroxide aqueous solution. After organic solvents were evaporated, the resultant precipitate was taken out. Eighty milliliters of a mixture of acetone and ethanol (1:1, v/v) was added to dissolve the precipitate, and acetone was evaporated to re-precipitate the product. This purification of the product was repeated twice. Although the final precipitate contained pure PLA/pyrene (1:1, mol/mol) conjugate and PLA, it was named PLA-pyrene, and used in the following experiments without further purification.

2.5. ^{1}H NMR spectroscopy and gel permeation chromatography

The chemical structures of PLA derivatives were confirmed from ^{1}H NMR spectra obtained with a JEOL JNM-GX270 spectrometer (JEOL, Japan). The degree of polymerization of the PLA moiety in the PLA derivatives was calculated from ^{1}H NMR spectra by comparing the integrated intensity of the methine proton of the terminal lactic group of the PLA chain to that of the methine proton of the inside lactic groups of the PLA chain. The number-average molecular weight (MWn) was also calculated using the degree of polymerization. The proportion of the diethylacetal, formyl or MeO-PEG(*N*) group introduced into PLA was calculated based on the ^{1}H NMR spectrum; that is, the extent of substitution was calculated by comparing the integrated intensity of the specific proton of each moiety with that of the methine proton of the terminal lactic group of the PLA chain. GPC was performed at room temperature to purify the polymer products. As reported previously (Sasatsu et al., 2006), the GPC system using a column of GPC K-800 (8 mm inner diameter × 300 mm long; Shodex, Japan) or GPC K-2003 (20 mm inner diameter × 300 mm long; Shodex, Japan) with chloroform as an elution solvent was used for the purification of PLA derivatives. A Shimadzu LC-6AD equipped with a refractive index detector (Shimazu RID-10A) was used. The flow rates of the elution solvent were 1 and 3.5 mL/min for GPC K-800 and GPC K-2003, respectively. Several polystyrenes (PSs) of known MW (Showa Denko K.K., Japan) were used as standard markers for MW.

2.6. Preparation of PLA-pyrene-loaded nanoparticles

PLA-pyrene-loaded nanoparticles were prepared using PLA–(MeO-PEG). Plain nanoparticles were prepared by the solvent diffusion method as follows. PLA–(MeO-PEG) (30 mg) was dissolved in a mixture of 1 mL of acetone and 0.5 mL of ethanol, and dripped gradually into 2.5 mL of water stirred gently. Then, an aqueous suspension of nanoparticles was obtained by evaporation of the organic solvents at 18 °C under reduced pressure. PLA-pyrene-loaded nanoparticles were prepared as follows. PLA–(MeO-PEG) (30 mg) and PLA-pyrene (9 mg) were dissolved in a mixture of 1 mL of acetone and 0.5 mL of ethanol, then dripped into 2.5 mL of water stirred gently. The organic solvent was evaporated at 18 °C under reduced pressure to obtain a suspension of nanoparticles. The nanoparticles were purified by gel-filtration with a Sephadex G-50 column (2.5 cm × 15 cm) using 0.45% (w/v) NaCl aqueous solution as an elution solvent. The eluted nanoparticles were characterized for the content and incorporation efficiency of PLA-pyrene. The incorporation efficiency was calculated as follows.

$$\text{Incorporation efficiency}\,(\%) = 100 \times \frac{\text{observed drug content}}{\text{ideal drug content}}$$

The content and incorporation efficiency of PLA-pyrene in the nanoparticles were examined by spectrophotometric absorption at 400 nm after their dissolution in acetonitrile. Furthermore, after the nanoparticles were dissolved in $CDCl_3$, a specified amount of 4-methoxyacetophenone was added, and the mixture was checked by ^{1}H NMR spectroscopy. The amount of polymer was determined by comparing the integrated intensity of the methine proton of the PLA chain and that of the methyl proton of the acetyl group of 4-methoxyacetophenone, which also gave the recovery of the polymer (PLA and PLA–(MeO-PEG)) in the nanoparticles.

2.7. In vitro characterization

The size of the nanoparticles was measured using an ELS-800 dynamic light scattering apparatus (Otsuka Electronic Co., Ltd., Japan) after their aqueous suspension was diluted adequately with water. The morphological examination of nanoparticles was performed by transmission electron microscopy (TEM) using a JEOL JEM-1011 transmission electron microscope (JEOL, Japan) after the nanoparticles were stained using a 3% (w/v) uranyl acetate aqueous solution and placed on copper grids. The release of PLA-pyrene from the nanoparticles was investigated in vitro. PLA-pyrene-loaded nanoparticles were incubated at three different particle concentrations of 84, 210 and 420 μg/mL in a PBS–EtOH (7:3, v/v) mixture or at the particle concentrations of 210 μg/mL in a PBS-normal mouse plasma (1:1, v/v) mixture at 100 strokes per min at 37 °C. At 1, 4 and 24 h after the start of incubation, the samples were taken and centrifuged at 40,000 rpm for 20 min, and the supernatant was adequately diluted, and fluorescence was measured using a JASCO FP-777 spectrofluorometer (JASCO, Japan) with excitation and emission wavelengths of 400 and 438 nm, respectively, to determine the amount of PLA-pyrene and its segments released.

2.8. Biodistribution experiments

PLA-pyrene-loaded nanoparticles suspended in 0.45% (w/v) NaCl, were injected intravenously as a bolus via a tail vein into normal mice. The dose was 20 mg nanoparticles/kg. At 1, 8 and 24 h after the injection, the mice were sacrificed by dislocation of the cervical vertebrae, blood was taken from the heart using a heparinized syringe, and the kidney, spleen, lung and liver were excised. After plasma was obtained by centrifugation of the blood at 3000 rpm for 10 min, 1 mL of acetone or acetonitrile was added to 0.1 mL of plasma. After the mixture was stirred with a vortex mixer for 3 min, it was centrifuged at 3000 rpm for 15 min to obtain the supernatant. Each excised organ was wiped with filter paper, and then put in saline of the same weight, and the mixture was homogenized using a glass homogenizer with a Teflon pestle. The homogenate was diluted 5.5-fold (v/v) by the addition of acetone or acetonitrile, and the resultant mixture was stirred with a vortex mixer for 3 min. The mixture was centrifuged at 3000 rpm for 15 min to obtain the supernatant. The supernatant was diluted adequately with the same organic solvent and measured fluorometrically using a JASCO FP-777 spectrofluorometer (JASCO, Japan), and was measured at the excitation and emission wavelengths of 400 nm and 438 nm, respectively. The value obtained by the subtraction of the fluorescence of the blank sample from that of the tested sample was calculated as a net fluorescence from the probe. Moreover, PLA-pyrene-loaded nanoparticles were injected at the same dose (20 mg nanoparticles/kg) intravenously as a bolus via the tail vein into tumor-bearing mice 7 d after inoculation. Plasma and other organs were collected at 1, 8, 24 and 48 h after injection and the following operation was performed in the same manner as in normal mice.

Recovery experiments were performed by addition of specified amounts of PLA-pyrene-loaded nanoparticles to fresh plasma or organs, treatment of the sample in the same manner as above and

Table 1
Characteristics of PLA–(MeO-PEG) obtained by reductive amination of PLA-aldehyde and MeO-PEG(*N*)

	MW of polymer[a]	Pure PLA/(MeO-PEG) (1:1) block copolymer (%, mol/mol)[a]
PLA–(MeO-PEG)(1)	16,700	56
PLA–(MeO-PEG)(2)	16,500	52

[a] Determined by ^{1}H NMR measurement in $CDCl_3$. The results are expressed as the mean ± S.D. (n = 3).

the fluorescence measurement. Calibration was performed using the net fluorescence calculated by the subtraction of the fluorescence of the blank sample from that of the sample containing the probe. The recovery ratios were estimated from the comparison of the concentration given by that calibration and the ideal concentration. The calibration could be completed well, and recovery ratios of the probe were 80–90% (data not shown) for all the tested tissues. The data were corrected with the recovery ratios.

3. Results and discussion

3.1. Preparation and characteristics of PLA–(MeO-PEG)

The obtained products were confirmed by ^{1}H NMR spectroscopy. Namely, the ^{1}H NMR spectrum of PLA-acetal (solvent, $CDCl_3$) were obtained as shown previously (Sasatsu et al., 2005), and the structure of PLA-aldehyde was also confirmed from the disappearance of diethylacetal-specific protons of PLA-acetal (1.1 ppm (triplet), 3.2–3.7 ppm (mlutiplet), 4.47 ppm (triplet) in $CDCl_3$) and generation of the formyl proton (9.74 ppm (singlet) in $CDCl_3$). Finally, two lots of PLA–(MeO-PEG) were obtained and used in this study (Table 1). Their MWn and substitution degree of MeO-PEG were obtained from ^{1}H NMR spectra (solvent, $CDCl_3$), in which relative integrated intensities for specific protons, appearing at chemical shifts of 3.61 ppm (PEG–C$\underline{H_2}$–C$\underline{H_2}$–O–: s), 4.32 ppm (terminal lactic group –COC$\underline{H}$(OH)C$\underline{H_3}$: q, J = 7 Hz) and 5.03–5.30 ppm (inside lactic group –COC$\underline{H}$(CH_3)O–: m), were 99/1/216 and 93/1/215 for PLA–(MeO-PEG)(1), PLA–(MeO-PEG)(2), respectively. The MWns of PLA–(MeO-PEG)(1) and PLA–(MeO-PEG)(2) were 16,700 and 16,500, respectively. The substitution degrees of MeO-PEG(*N*) were 56 and 52% (mol/mol), respectively. A GPC elution profile of PLA–(MeO-PEG))(1) (peak top, 11.8 min) is shown in Fig. 2, indicating that PLA–(MeO-PEG) was completely separated from MeO-PEG(*N*) (peak top, 21.1 min). PLA–(MeO-PEG)

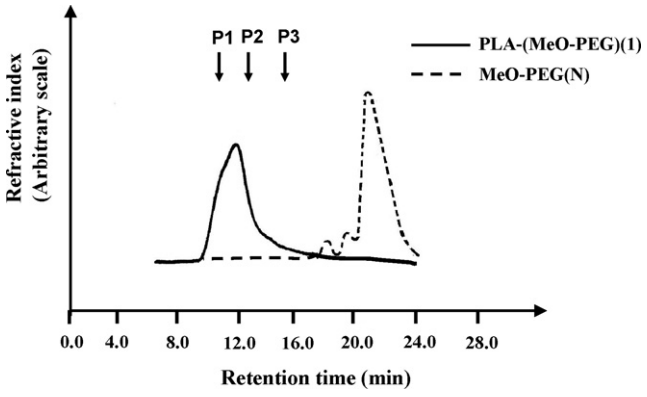

Fig. 2. Gel permeation profiles of PLA–(MeO-PEG)) and Me-PEG (*N*). A column, GPC K-2003, was used with chloroform as an eluent at the flow rate of 3.5 mL/min. Each sample solution in chloroform (0.2 mL) with the concentration of 10 mg/mL was injected. P1, P2 and P3 show the elution peak positions of PS satandards with the molecular weight of 28.6, 10.9 and 3.0 kDa, respectively.

Table 2
Characteristics of PLA-pyrene obtained by reductive amination of PLA-aldehyde and aminopyrene

	MW of polymer[a]	Pyrene/PLA[a] (%, mol/mol)
PLA-pyrene	10,500 ± 400	37.5 ± 1.7

[a] Determined by ^{1}H NMR measurement in $CDCl_3$. The results are expressed as the mean ± S.D. (n = 3).

(2) also exhibited the similar patterns (data not shown). Thus, the PLA–(MeO-PEG) MW given by GPC using standard markers are almost consistent with Mn obtained by ^{1}H NMR spectra.

3.2. Preparation and characteristics of PLA-pyrene

For PLA-pyrene, the MWn and pyrene substitution degree were calculated from ^{1}H NMR spectra (solvent, $CDCl_3$), in which relative integrated intensities for the specific protons, appearing at the chemical shifts of 4.32 (terminal lactic group –COC$\underline{H}$(OH)C$\underline{H_3}$: q, J = 7 Hz) and 5.03–5.30 (inside lactic group –COC$\underline{H}$(CH3)O–: m) and 7.50–8.60 (pyrene aromatic group protons: m), were 1, 143 ± 2.6, and 3.0 ± 0.1 (each, n = 3) for PLA-pyrene. Using PLA-aldehyde with 50% of formyl group/PLA (mol/mol), the reaction efficiency was approx. 70%. The chemical characteristics are shown in Table 2. The UV–vis absorption analyses of PLA-pyrene showed almost the same substitution degree as that obtained by ^{1}H NMR, indicating the UV–vis absorption was available for the determination of the PLA-pyrene amount. The fluorescence spectrum of PLA-pyrene excited at 400 nm in acetonitrile is shown in Fig. 3.

3.3. In vitro particle characteristics

Plain nanoparticles were prepared with the solvent diffusion method using PLA–(MeO-PEG) as a drug carrier. The mean size was 112 nm measured by the dynamic light scattering method. Their TEM micrograph showed similar size and spherical shape (Fig. 4). The particle characteristics of PLA-pyrene-loaded nanoparticles produced using PLA–(MeO-PEG)(1) and (2) are shown in

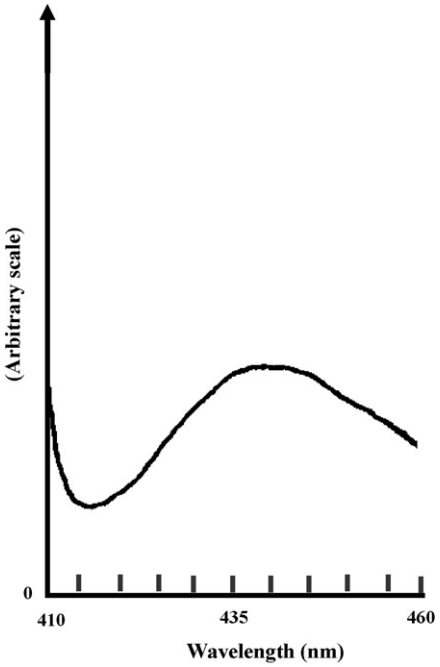

Fig. 3. Fluorescence spectrum of PLA-pyrene.

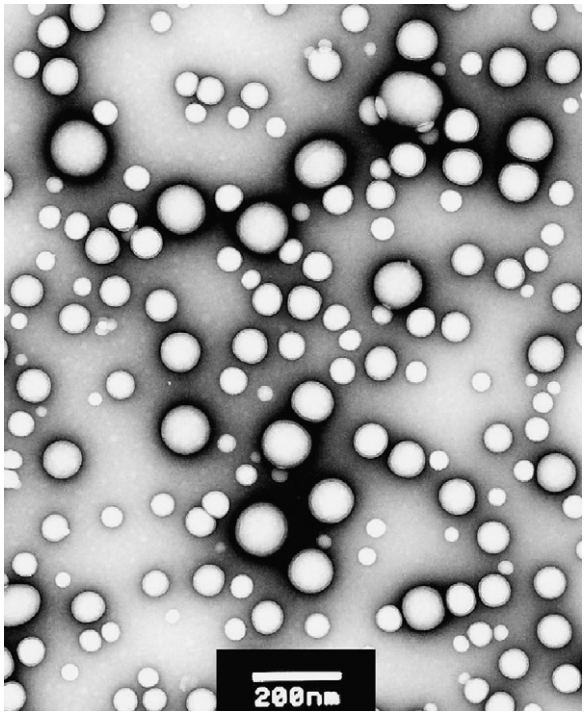

Fig. 4. TEM photomicrographs of plain PLA–(MeO-PEG)) nanoparticles obtained by solvent diffusion method. The white bar is 200 nm long.

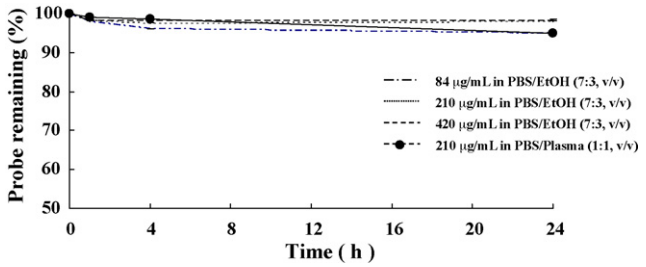

Fig. 5. Maintenance of the probe in PLA-pyrene-loaded nanoparticles during the incubation at 37 °C at a particle concentration of 84 μg/mL, 210 μg/mL and 420 μg/mL in the PBS/EtOH (7: 3, v/v) mixture or at a particle concentration of 210 μg/mL in the PBS/plasma (1:1, v/v) mixture. The results are expressed as the mean ± S.D. (n = 3).

Table 3. The size of these nanoparticles was smaller in PLA-pyrene NP(1) than in PLA-pyrene NP(2). The loadings of the probe were similar in both nanoparticles. The MWn of PLA–(MeO-PEG)(1) was almost the same as that of PLA–(MeO-PEG)(2), but the MeO-PEG (*N*) substitution degree was slightly higher in PLA–(MeO-PEG)(1) than in PLA–(MeO-PEG)(2). According to Bazile et al. (1995), when nanoparticles were produced with a mixture of a similar diblock copolymer, MeO-PEG–PLA (MW 12,000 or 32,000), and PLA (MW 60,000), the particle size became smaller with the increase in the ratio of MeO-PEG–PLA to PLA, which was similar to the present result. Therefore, the difference in the ratio of MeO-PEG(*N*)-substituted PLA to non-substituted PLA was considered to influence the particle size difference. The particle size was suitable for the EPR effect. The diameter of PLA-pyrene-loaded nanoparticles tended to be larger than plain nanoparticles. Incorporation efficiency of PLA-pyrene was around 100% or a little more, indicating the probe could be incorporated very efficiently. This was considered to be because PLA-pyrene had almost the same chemical structure as PLA chain of the nanoparticle core.

The release of the probe from nanoparticles was examined in vitro by incubation in a mixture of PBS and EtOH (7:3, v/v) and a mixture of PBS and normal mouse plasma (1:1, v/v) at 37 °C (Fig. 5). In the former mixture, the concentration given by the complete release was much lower than the solubility of PLA-pyrene. PLA-pyrene was retained almost completely in the nanoparticles 24 h after the incubation in the PBS–EtOH mixture. This supported that PLA-pyrene would behave as fluorescence–labeled PLA. Furthermore, the amount of probe remaining in the nanoparticles was 95% (w/w) 24 h after the incubation in the PBS–plasma mixture. The particles precipitated after ultracentrifugation of the samples kept the probe color within them very well. Recently, studies on adsorption of plasma proteins to micro- or nanoparticles composed of PLA or PLA/PEG-PLA mixture have been reported (Allémann et al., 1997; Lacasse et al., 1998; Zambaux et al., 1999; Gref et al., 2000; Atthoff and Hilborn, 2007). The plasma proteins are adsorbed quickly to such particles (Allémann et al., 1997; Zambaux et al., 1999; Gref et al., 2000), and particle core remains long, that is, the degradation of the matrix by the hydrolysis of the esters in physiological conditions takes weeks- or months long period (Ogawa et al., 1988; Yoo et al., 1999). These indicated that the PLA of the particles stably remains in the core. Considering that PLA-pyrene, structurally similar to PLA, surely behaves similarly to PLA, the results in the PBS/plasma mixture were considered to represent very slight release of PLA-pyrene or its segments, and not to show apparent release following precipitation by interaction between plasma proteins and released PLA-pyrene or its segments. This would be made clear by washing adsorbed proteins with a protein solubilizing solution (Zambaux et al., 1999; Gref et al., 2000) and resultant analysis of chemical characteristics of the resultant precipitate, including the probe amount, which will be a future subject. These in vitro studies suggested that PLA-pyrene should be retained stably in the nanoparticles and that PLA-pyrene could be a good probe of the nanoparticles themselves. Yamamoto et al. (2002) reported on the chain exchange among the PEG-PLA micelles using MeO-PEG–PLA-pyrene and lactose-PEG-PLA. MeO-PEG–PLA-pyrene was used as labeled MeO-PEG–PLA. The present PLA-pyrene was also developed as labeled PLA, and was considered to be stably retained in the nanoparticles and to behave as a probe of the nanoparticles themselves.

3.4. Biodistribution of nanoparticles after i.v. administration

First, PLA-pyrene-loaded nanoparticles were examined for biodistribution in normal mice. PLA-pyrene-loaded nanoparticles with the mean size of 162 nm, PLA-pyrene NP(1) (Table 3), were used for normal mice. Their size was very similar to that of DiD-loaded nanoparticles (mean size, 154 nm), which was previously reported (Sasatsu et al., 2006). The biodisposition profiles of the probe in plasma and major organs are shown in Fig. 6. For the initial period, PLA-pyrene-loaded nanoparticles showed high plasma levels of the probe, and distribution in the organs was low. The

Table 3
Particle characteristics of fluorescence probe-loaded PLA–(MeO-PEG) nanoparticles obtained by solvent diffusion method

	PLA–(MeO-PEG)	Mean diameter (nm)	Amiopyrene content[a] (%, w/w)	Incorporation efficiency (%)
PLA-pyrene NP(1)	PLA–(MeO-PEG)(1)	161.9 ± 7.5	0.16 ± 0.00	106.7 ± 2.7
PLA-pyrene NP(2)	PLA–(MeO-PEG)(2)	221.6 ± 9.6	0.18 ± 0.05	114.6 ± 29.0

[a] This is shown as weight % of aminopyrene in the nanoparticles. The results are expressed as the mean ± S.D. (*n* = 3).

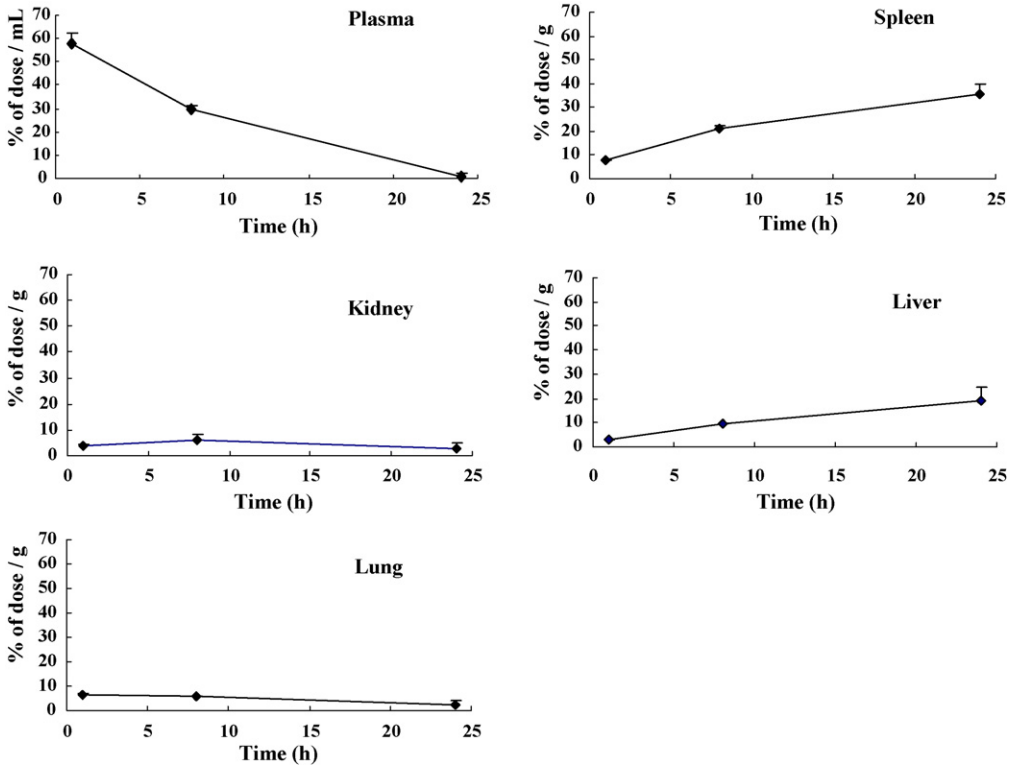

Fig. 6. Biodistribution profiles of the probe in plasma and organs after i.v. injection of PLA-pyrene-loaded nanoparticles to nomal mice at a dose of 20 mg/kg. The results are expressed as the mean ± S.E. (n = 4).

probe was eliminated gradually from the plasma, and was accumulated gradually in spleen and liver. The accumulation in kidney and lung was slight. When compared with the biodistribution of DiD previously reported (Sasatsu et al., 2006), the level of PLA-pyrene was higher in plasma and lower in the liver and spleen. As the particle size and dose are almost the same between PLA-pyrene NP(1) and the DiD-loaded nanoparticles, the size and dose were not the reason for the difference in both biodistribution profiles. Although DiD was stably retained in the nanoparticles in vitro as stated previously (Sasatsu et al., 2006), DiD has characteristics to be easily adsorbed by red blood cells, and the direct transfer of DiD from PLA nanocapsules to cells by collision/adsorption was suggested to happen (Mosqueira et al., 1999). On the other hand, since PLA-pyrene was structurally similar to PLA, PLA-pyrene was considered to behave similarly to PLA that was localized stably in the hydrophobic core. These different features might lead to the difference between both the biodistribution profiles. However, in order to make this point more clearly, those nanoparticles will have to be examined more for the stability in biological media and in the presence of cells.

In addition, we examined the potential of nanoparticles for tumor passive targeting using sarcoma-180 solid tumor-bearing mice. PLA-pyrene nanoparticles with the size of 220 nm, PLA-pyrene NP(2) (Table 3), were used, because the nanoparticles, which we had been tested for drug-loaded nanoparticles before, had a particle size of 200–250 nm (Miura et al., 2004; Kunii et al., 2007). The tissue distribution profiles are shown in Fig. 7. At 1 h after administration, the plasma level of the probe was high with 40% of the dose or more and the tumor level was a few % of the dose. The tumor concentration of the probe increased at 8 h, which suggested that nanoparticles should accumulate in tumors. The probe concentration in tumors was maintained fairly high until 48 h. The elimination from the plasma and accumulation into spleen were greater than those in normal rats stated above. This might be mainly due to the difference in particles size, and tumor accumulation was also considered to contribute to the faster elimination of the nanoparticles from the plasma. The ratio of tumor concentration to plasma concentration increased with time as shown in Fig. 8, in particular, at 48 h, the tumor/plasma ratio reached more than 10, indicating the good tumor targeting abil-

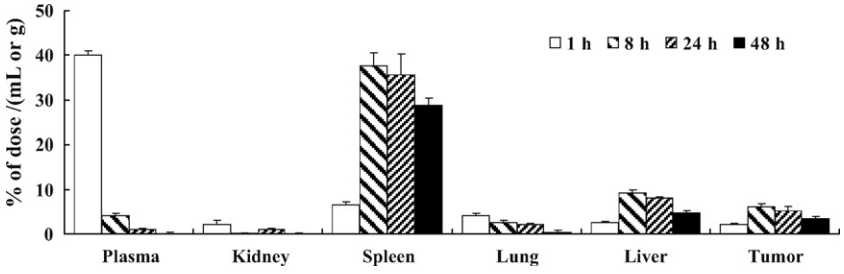

Fig. 7. Tissue distribution profiles of the probe after i.v. injection of PLA-pyrene-loaded nanoparticles to sarcoma-180 solid tumor-bearing mice at a dose of 20 mg particles/kg. The results are expressed as the mean ± S.E. (n = 4).

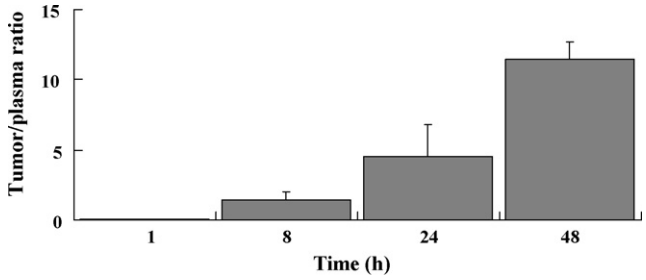

Fig. 8. Tumor localization of the probe after i.v. injection to sarcoma-180 solid tumor-bearing mice at a dose of 20 mg particles/kg. The injection was performed 7 d after inoculation. The results are expressed as the mean ± S.E. (n = 3–4).

ity of the nanoparticles. These tumor localization properties was considered to be due to accumulation of the nanoparticles based on the enhanced permeability and retention (EPR) effect in tumor tissues (Matsumura and Maeda, 1986; Jain, 1987; Yokoyama et al., 1991; Woodle and Lasic, 1992; Unezaki et al., 1995; Zhang et al., 1997). It was demonstrated that PLA–(MeO-PEG) nanoparticles of 220 nm should have potential to display passive drug targeting to tumors, though nanoparticles also showed a tendency to be distributed toward the spleen. Similar features were observed about the CPT distribution after i.v. administration of CPT-loaded PEG-PLA nanoparticles with a similar size (Miura et al., 2004), which was probably because of the same reason.

4. Conclusion

A novel probe, PLA-pyrene, was prepared by reductive amination of PLA-aldehyde and aminopyrene. This probe was retained stably in the nanoparticles in a sink condition and at the presence of plasma. In addition, considering the structure of PLA-pyrene was like PLA, it was suggested that the probe should behave similarly to core PLA chain and represent the biodistribution of nanoparticles themselves. The probe was eliminated gradually from the plasma, and accumulated into spleen and liver to a fair extent, supporting the nanoparticles should be useful to exhibit EPR effect. PLA–(MeO-PEG) nanoparticles with the mean size of 220 nm were accumulated in tumors and retained there for a long time, suggesting that the nanoparticles should be useful as a carrier for passive tumor targeting.

References

Abraham, S.A., Waterhouse, D.N., Mayer, L.D., Cullis, P.R., Madden, T.D., Bally, M.B., 2005. The liposomal formulation of doxorubicin. Methods Enzymol. 391, 71–97.

Allémann, E., Gravel, P., Leroux, J.C., Balant, L., Gurny, R., 1997. Kinetics of blood component adsorption on poly(D,L-lactic acid) nanoparticles: evidence of complement C3 component involvement. J. Biomed. Mater. Res. 37, 229–234.

Atthoff, B., Hilborn, J., 2007. Protein adsorption onto polyester surfaces: is there a need for surface activation? J. Biomed. Mater. Res. B Appl. Biomater. 80, 121–130.

Bazile, D., Prud'homme, C., Bassoullet, M.T., Marlard, M., Spenlehauer, G., Veillard, M., 1995. Stealth Me.PEG-PLA nanoparticles avoid uptake by the mononuclear phagocytes system. J. Pharm. Sci. 84, 493–498.

Brannon-Peppas, L., Blanchette, J.O., 2004. Nanoparticle and targeted systems for cancer therapy. Adv. Drug Deliv. Rev. 56, 1649–1659.

Charrois, G.J., Allen, T.M., 2004. Drug release rate influences the pharmacokinetics, biodistribution, therapeutic activity, and toxicity of pegylated liposomal doxorubicin formulations in murine breast cancer. Biochim. Biophys. Acta 1663, 167–177.

Dunn, S.E., Coombes, A.G.A., Garnett, M.C., Davis, S.S., Davies, M.C., Illum, L., 1997. In vitro cell interaction and in vivo biodistribution of poly(lactide-co-glycolide) nanospheres surface modified by poloxamer and poloxamine copolymers. J. Control. Release 44, 65–76.

Gref, R., Lück, M., Quellec, P., Marchand, M., Dellacherie, E., Harnisch, S., Blunk, T., Müller, R.H., 2000. 'Stealth' corona-core nanoparticles surface modified by polyethylene glycol (PEG): influences of the corona (PEG chain length and surface density) and of the core composition on phagocytic uptake and plasma protein adsorption. Colloids Surf. B Biointerfaces 18, 301–313.

Gref, R., Minamitake, Y., Peracchia, M.T., Trubetskoy, V., Torchilin, V., Langer, R., 1994. Biodegradable long-circulating polymeric nanospheres. Science 263, 1600–1603.

Ishida, O., Maruyama, K., Sasaki, K., Iwatsuru, M., 1999. Size-dependent extravasation and interstitial localization of polyethyleneglycol liposomes in solid tumor-bearing mice. Int. J. Pharm. 190, 49–56.

Jain, R.K., 1987. Transport of molecules across tumor vasculature. Cancer Metastasis Rev. 6, 559–593.

Kanke, M., Simmons, G.H., Weiss, D.L., Bivins, B.A., DeLuca, P.P., 1980. Clearance of 141Ce-labeled microspheres from blood and distribution in specific organs following intravenous and intraarterial administration in beagle dogs. J. Pharm. Sci. 69, 755–762.

Kunii, R., Onishi, H., Machida, Y., 2007. Preparation and antitumor characteristics of PLA/(PEG-PPG-PEG) nanoparticles loaded with camptothecin. Eur. J. Pharm. Biopharm. 67, 9–17.

Lacasse, F.X., Filion, M.C., Phillips, N.C., Escher, E., McMullen, J.N., Hildgen, P., 1998. Influence of surface properties at biodegradable microsphere surfaces: effects on plasma protein adsorption and phagocytosis. Pharm. Res. 15, 312–317.

Machida, Y., Onishi, H., Kato, Y., Machida, Y., 2003. Efficacy of irinotecan-containing nanoparticles prepared using poly(DL-lactic acid) and poly(ethylene glycol)-block-poly(propylene glycol)-block-poly(ethylene glycol) against M5076 tumor in the early liver metastatic stage. S.T.P. Pharma Sci. 13, 225–230.

Matsumura, Y., Maeda, H., 1986. A new concept for macromolecular therapeutics in cancer chemotherapy: mechanism of tumoritropic accumulation of proteins and the antitumor agent smancs. Cancer Res. 46, 6387–6392.

Miura, H., Onishi, H., Sasatsu, M., Machida, Y., 2004. Antitumor characteristics of methoxypolyethylene glycol-poly(DL-lactic acid) nanoparticles containing camptothecin. J. Control. Release 97, 101–113.

Mosqueira, V.C., Legrand, P., Gref, R., Heurtault, B., Appel, M., Barratt, G., 1999. Interactions between a macrophage cell line (J774A1) and surface-modified poly (D,L-lactide) nanocapsules bearing poly(ethylene glycol). J. Drug Target. 7, 65–78.

Nagasaki, Y., Yasugi, K., Yamamoto, Y., Harada, A., Kataoka, K., 2001. Sugar-installed block copolymer micelles: their preparation and specific interaction with lectin molecules. Biomacromolecules 2, 1067–1070.

Nguyen, C.A., Allemann, E., Schwach, G., Doelker, E., Gurny, R., 2003. Cell interaction studies of PLA-MePEG nanoparticles. Int. J. Pharm. 254, 69–72.

Ogawa, Y., Okada, H., Yamamoto, M., Shimamoto, T., 1988. In vivo release profiles of leuprolide acetate from microcapsules prepared with polylactic acids or copoly(lactic/glycolic) acids and in vivo degradation of these polymers. Chem. Pharm. Bull. (Tokyo) 36, 2576–2581.

Onishi, H., Machida, Y., Machida, Y., 2003. Antitumor properties of irinotecan-containing nanoparticles prepared using poly(DL-lactic acid) and poly(ethylene glycol)-block-poly(propylene glycol)-block-poly(ethylene glycol). Biol. Pharm. Bull. 26, 116–119.

Sasatsu, M., Onishi, H., Machida, Y., 2005. Preparation of a PLA-PEG block copolymer using a PLA derivative with a formyl terminal group and its application to nanoparticulate formulation. Int. J. Pharm. 294, 233–245.

Sasatsu, M., Onishi, H., Machida, Y., 2006. In vitro and in vivo characterization of nanoparticles made of MeO-PEG amine/PLA block copolymer and PLA. Int. J. Pharm. 317, 167–174.

Shenoy, V.S., Vijay, I.K., Murthy, R.S., 2005. Tumour targeting: biological factors and formulation advances in injectable lipid nanoparticles. J. Pharm. Pharmacol. 57, 411–422.

Sugibayashi, K., Morimoto, Y., Nadai, T., Kato, Y., Hasegawa, A., Arita, T., 1979. Drug-carrier property of albumin microspheres in chemotherapy. II. Preparation and tissue distribution in mice of microsphere-entrapped 5-fluorouracil. Chem. Pharm. Bull. 27, 204–209.

Tabata, Y., Murakami, Y., Ikada, Y., 1998. Tumor accumulation of poly(vinyl alcohol) of different sizes after intravenous injection. J. Control. Release 50, 123–133.

Unezaki, S., Maruyama, K., Ishida, O., Suginaka, A., Hosoda, J., Iwatsuru, M., 1995. Enhanced tumor targeting and improved antitumor activity of doxorubicin by long-circulating liposomes containing amphipathic poly(ethylene glycol). Int. J. Pharm. 126, 41–48.

Woodle, M.C., Lasic, D.D., 1992. Sterically stabilized liposomes. Biochim Biophys Acta. 1113, 171–199.

Yang, S.C., Lu, L.F., Cai, Y., Zhu, J.B., Liang, B.W., Yang, C.Z., 1999. Body distribution in mice of intravenously injected camptothecin solid lipid nanoparticles and targeting effect on brain. J. Control. Release 59, 299–307.

Yamamoto, Y., Yasugi, K., Harada, A., Nagasaki, Y., Kataoka, K., 2002. Temperature-related change in the properties relevant to drug delivery of poly(ethylene glycol)-poly(D,L-lactide) block copolymer micelles in aqueous milieu. J. Control. Release 82, 359–371.

Yokoyama, M., Okano, T., Sakurai, Y., Ekimoto, H., Shibazaki, C., Kataoka, K., 1991. Toxicity and antitumor activity against solid tumors of micelle-forming polymeric anticancer drug and its extremely long circulation in blood. Cancer Res. 51, 3229–3236.

Yoo, H.S., Oh, J.E., Lee, K.H., Park, T.G., 1999. Biodegradable nanoparticles containing doxorubicin-PLGA conjugate for sustained release. Pharm. Res. 16, 1114–1118.

Zambaux, M.F., Bonneaux, F., Gref, R., Dellacherie, E., Vigneron, C., 1999. MPEO-PLA nanoparticles: effect of MPEO content on some of their surface properties. J. Biomed. Mater. Res. 44, 109–115.

Zhang, X., Burt, H.M., Mangold, G., Dexter, D., Von Hoff, D., Mayer, L., Hunter, W.L., 1997. Anti-tumor efficacy and biodistribution of intravenous polymeric micellar paclitaxel. Anticancer Drugs 8, 696–701.